JOC The Journal of Organic Chemistry

pubs.acs.org/joc Article

Electro-reductive Fragmentation of Oxidized Lignin Models

Cheng Yang, Gabriel Magallanes, Stephen Maldonado, and Corey R. J. Stephenson*

Cite This: https://doi.org/10.1021/acs.joc.1c00346 Read Online

ACCESS | Metrics & More | Article Recommendations | Supporting Information

ABSTRACT: Lignin provides a potential sustainable source for production of electron-rich aromatic compounds. Recently, electrochemical lignin degradation via an oxidation/reduction sequence under mild conditions has garnered much attention within the lignin community, as electrochemistry simplifies redox reactions and offers an electron source/sink for synthesis without using stoichiometric oxidants or reductants. This paper describes a fundamental approach for the electrochemical fragmentation of the primary connection in native lignin, β-O-4. Potential-controlled electrolysis enables selective reduction and provides fragmentation products and/or coupling products in isolated yields of 59−92%.

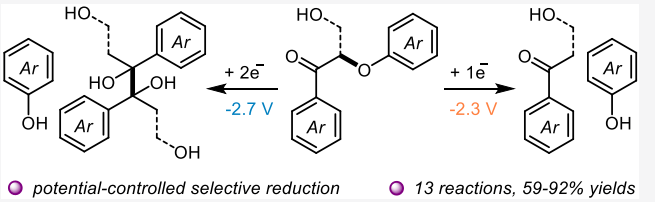

Downloaded via UNIV INDUSTRIAL DE SANTANDER on August 10, 2021 at 21:44:50 (UTC).
See https://pubs.acs.org/sharingguidelines for options on how to legitimately share published articles.

INTRODUCTION

Natural polymer lignin is a potential candidate as a renewable chemical source.[1] Lignin represents the most abundant stockpile of aromatic functional groups in nature and is potentially a well of highly valuable electron-rich aromatic chemicals (e.g., vanillin).[2] However, lignin is difficult to fragment into usable monomers due to its complex connectivity.[3] Lignin features an irregular pattern of methoxy-substituted aromatic groups linked together via aliphatic C−C and C−O bonds.[4] Despite a large content of weak C−O connections in the structure,[5] lignin surprisingly cannot be broken down by hydrolysis. Instead, acid hydrolysis drives rapid repolymerization through the formation of stronger C−C bonds via benzylic carbocation attack (Figure 1A).[6] This aspect in the reactivity of lignin affords "natural protection" to plant cell walls, imparting durability and impermeability toward water. However, this aspect also makes energy-efficient lignin depolymerization extremely challenging.[7]

The β-O-4 motif, the most abundant connection in lignin, is often used as a model for methodology development, and its fragmentation strategies in the literature can be divided into two prominent categories: hydrogenolysis and selective deconstruction via oxidation/reduction. Hydrogenolysis generally requires the use of noble metals and harsh conditions such as high temperature and high pressure, resulting in a complex mixture of phenols, cyclic alcohols, cycloalkanes, etc.[8] In contrast, our lab seeks to explore selective and mild deconstruction of lignin, which is possible through a sequence of oxidation and reduction reactions. The β-O-4 structure contains two hydroxyl functional groups, a benzylic alcohol and an aliphatic alcohol (Figure 1A). Several examples of selective oxidation of these alcohols have appeared throughout the literature.[9] For example, our lab has developed a benzylic oxidation utilizing *N*-hydroxyphthalimide as an electrocata-

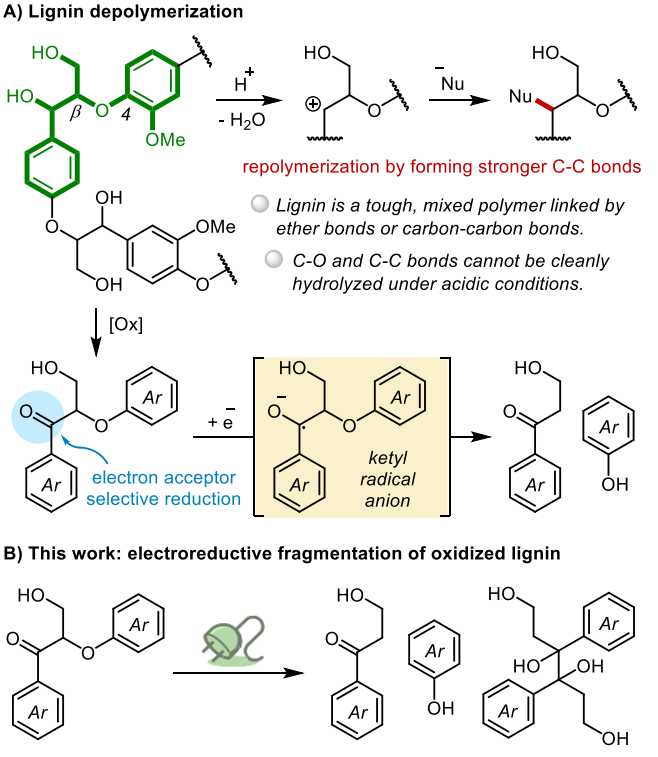

Figure 1. Depolymerization of oxidized lignin.

Special Issue: Electrochemistry in Synthetic Organic Chemistry

Received: February 11, 2021

© XXXX American Chemical Society

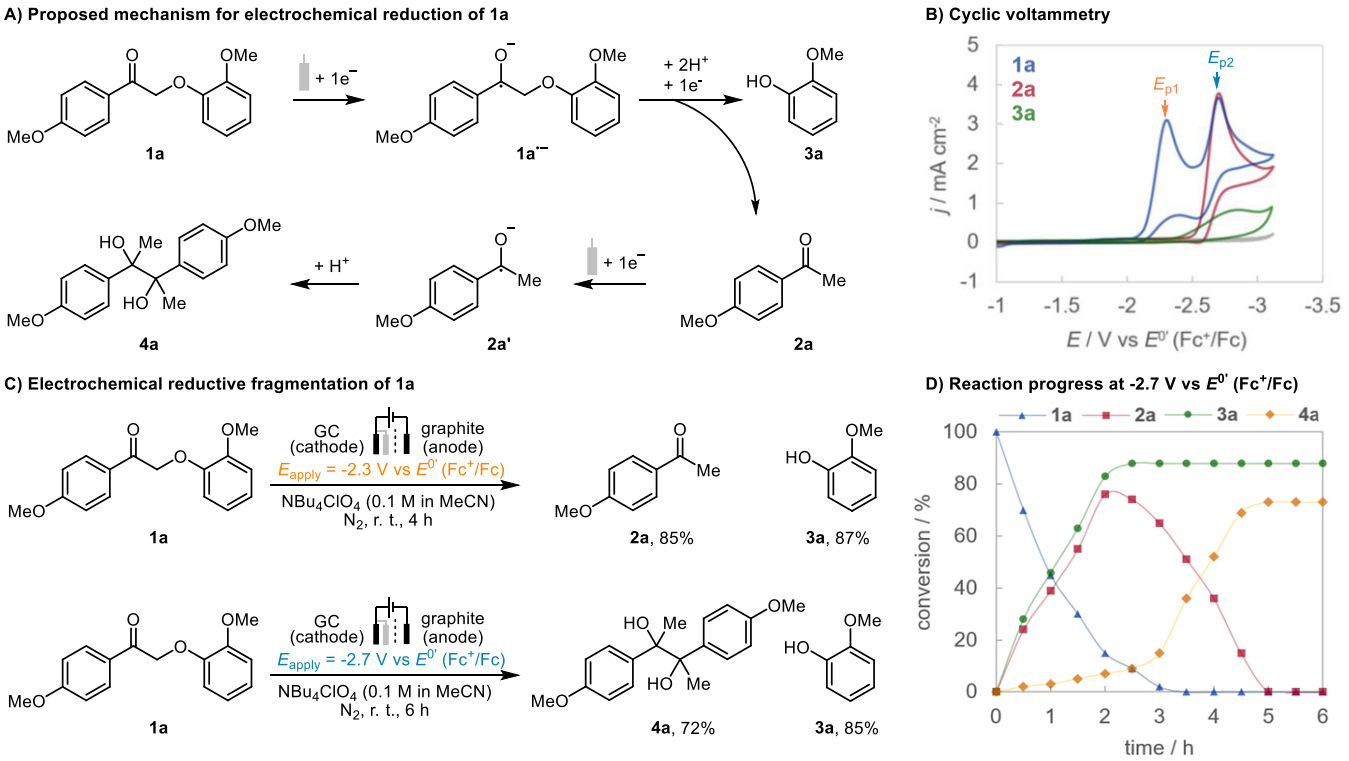

Figure 2. (A) Proposed mechanism for electrochemical reduction of **1a**. (B) Cyclic voltammograms for reduction of 10 mM **1a** (blue), **2a** (red), and **3a** (green) with 0.1 M NBu_4ClO_4 (background, gray) in degassed MeCN at 0.1 V s^{-1}. C) Conditions: **1a** (0.16 mmol, 20 mM), NBu_4ClO_4 (0.1 M in 8 mL MeCN), N_2 protection, glassy carbon cathode, graphite anode, $Ag/AgNO_3$ reference electrode, divided cell, constant potential control. Yields were determined by ^1H NMR using 1,3,5-trimethoxybenzene as internal standard. (D) Reaction progress at −2.7 V vs $E^{0\prime}$ (Fc^+/Fc) monitored by GC−MS.

lyst.[10] Such oxidation reactions introduce a good electron acceptor which allows facile fragmentation via a selective reduction. Reductive C−O fragmentation of benzylic-oxidized lignin involves the fragmentation of a ketyl radical anion intermediate to produce value-added building blocks, such as aromatic ketones and phenols.[9−13] Mechanistically, the fragmentation reaction entails a one-electron reduction of the ketone to initiate the C−O cleavage (Figure 1A). Toward this objective, this study utilizes the simplicity of electrochemistry to explore the fundamental aspects of *reductive* lignin fragmentation in an electrochemical cell.

Electrochemistry is a promising strategy for lignin depolymerization due to its unique advantages.[14] On one hand, continuous potential control can provide high selectivity for the desired deconstruction. On the other hand, paired electrolysis processes allow simultaneous generation of chemicals from both the oxidation and reduction reactions. For example, Moeller and co-workers have suggested the cathodic byproduct hydrogen gas, produced from a benzylic alcohol oxidation, can be used for hydrogenation reactions.[15] Most recent efforts toward lignin degradation from Moeller,[15] Waldvogel,[16] Stahl,[17] and our lab[10] have focused on electrochemical oxidation. Despite Hegg, Jackson, and co-workers' report on thio-assisted *β*-O-4 cleavage,[18] very few examples of *β*-O-4 reduction have been published. This paper expands our electrochemical lignin oxidation method and describes an electro-reductive fragmentation of oxidized lignin models (Figure 1B). In comparison to previously reported electro-reductive lignin cleavage without any preoxidation treatment,[19] reduction of oxidized lignin provides higher selectivity and high-yield production of defined aromatic molecules.

RESULTS AND DISCUSSION

Our previous study suggests that the selection of an appropriate proton source is critical to achieve high yields and high efficiency in this transformation.[12] In principle, an acid proton source can activate the ketone substrate and lower the reaction driving force. However, hydrogen evolution can also outcompete the desired lignin reduction reaction and decrease the overall rate. Thus, we sought initially to investigate the proton source effects on electrochemical lignin reduction. For preliminary validation and method development, this study focuses on a benzylic oxidized *β*-O-4 model substrate.

The study began with a current-controlled bulk electrolysis of oxidized *β*-O-4 model **1a** without any additives using a two-electrode, divided cell to prevent crossover between electrodes. By injecting 3 equiv of electrons into the solution, the reaction delivered the desired products **2a** and **3a** in 43% and 86% ^1H NMR yields, respectively. In addition, a pinacol dimer **4a** was observed in 41% ^1H NMR yield. The unexpected dimer suggests that the direct reduction of *β*-O-4 at a glassy carbon electrode proceeds differently from the similar photochemical reduction.[12] In addition to the absence of strong acid, evidence for extensive over-reduction of the product was collected for certain experimental conditions here. Experiments were performed to understand the mechanistic details that pertain to pinacol formation and reaction selectivity.

https://doi.org/10.1021/acs.joc.1c00346
J. Org. Chem. XXXX, XXX, XXX−XXX

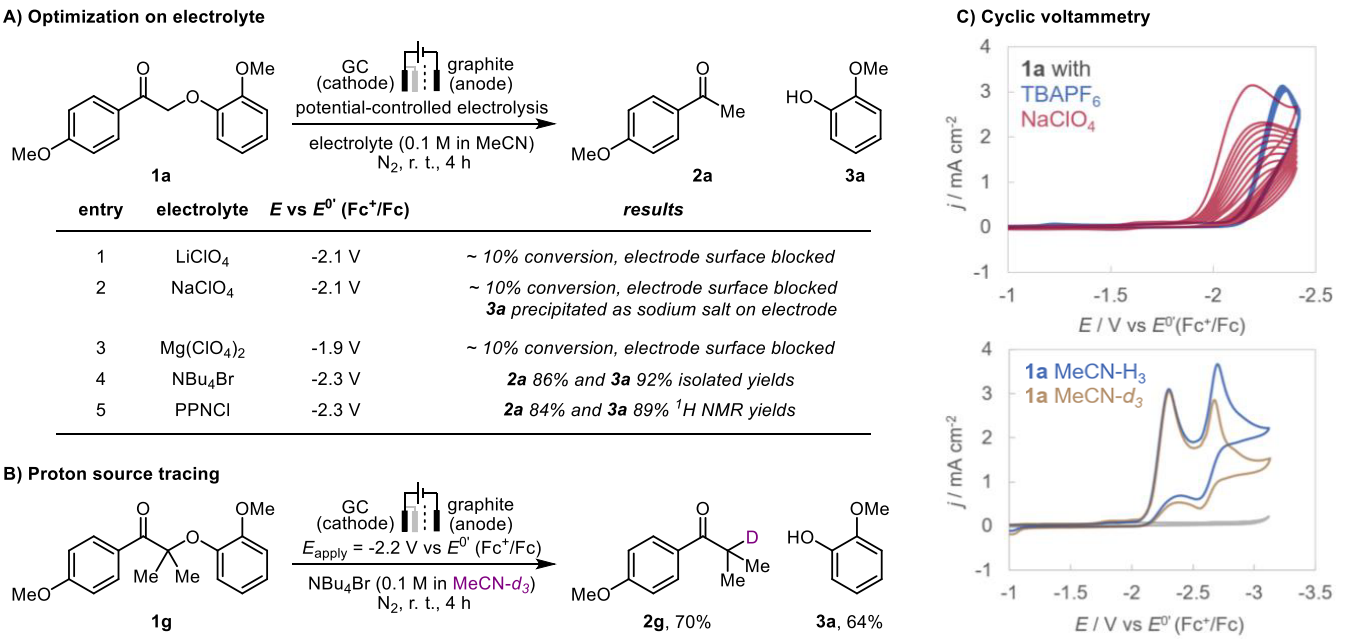

Figure 3. (A) Optimization of electrolyte. Conditions: **1a** (0.16 mmol, 20 mM), electrolyte (0.1 M in 8 mL MeCN), N_2 protection, glassy carbon cathode, graphite anode, $Ag/AgNO_3$ reference electrode, divided cell, constant potential control. Yields were determined by ^1H NMR using 1,3,5-trimethoxybenzene as internal standard. (B) Isotope labeling experiment performed in MeCN-d_3. (C) Cyclic voltammograms (top) for reduction of 10 mM **1a** with 0.1 M NBu_4ClO_4 (blue) an $NaClO_4$ (red) in degassed MeCN at 0.1 V s^{-1} for 20 cycles. Cyclic voltammograms (bottom) for reduction of 10 mM **1a** in degassed MeCN (blue) and MeCN-d_3 (yellow).

Cyclic voltammetric measurements for the reduction of **1a** revealed a subsequent two-electron transfer mechanism at a glassy carbon electrode within a solution of 0.1 M tetrabutylammonium perchlorate (NBu_4ClO_4) in degassed acetonitrile (MeCN) at 0.1 V s^{-1} (Figure 2A). In the presented potential range, the redox response for reduction of **1a** showed two sets of irreversible reduction waves. The second peak appeared at the same potential as the reduction of **2a** under the same conditions. Accordingly, the more positive peak at −2.3 V (E_{p1}, vs $E^{0\prime}$ (Fc^+/Fc)) was assigned to the formation of ketyl radical anion $\mathbf{1a}^{\bullet-}$.[20] This intermediate $\mathbf{1a}^{\bullet-}$ eventually could yield **2a** and **3a** via multiple possible mechanisms. Both mechanisms require the net transfers of one electron and two protons. In one path (path a), a hydrogen atom transfer and proton transfer could occur; whereas in another (path b), one electron transfer and two proton transfers could occur. At a more negative potential (E_{p2} = −2.7 V), the ketone fragmentation product **2a** was reduced[21] and subsequently formed pinacol **4a** via dimerization. Based on the ∼0.5 V peak separation in the voltammetry, we posit that these two reduction events can be selectively controlled, i.e., the further reduction of **2a** can be avoided by applying a potential less negative than −2.4 V.

To test our hypothesis, a series of three-electrode, potential-controlled bulk electrolyses of **1a** were performed in a solution of 0.1 M NBu_4ClO_4 in MeCN under air free conditions, avoiding concomitant oxygen reduction. Applying a potential of −2.2 V[22] gave fragmentation products **2a** and **3a** in 85% and 87% ^1H NMR yields, respectively. When a more negative potential of −2.7 V was applied, electrolysis led to the formation of pinacol coupling product **4a** and **3a** in 72% and 85% ^1H NMR yields, respectively. Integration of the chronocoulometric data (i.e., charge as a function of time) suggested that 1.3 equiv (19.7 Coulombs) and 1.4 equiv (21.4 Coulombs) of electrons passed through the cell, respectively.[23]

The noninteger equivalents implies that the conversion from $\mathbf{1a}^{\bullet-}$ to **2a** and **3a** occurs via multiple mechanisms, and path b possibly exists as a minor mechanism. Furthermore, reaction progress as monitored by GC−MS is presented in Figure 2D to elaborate the process of pinacol formation under more negative applied bias. In the first 2.5 h, **1a** was converted upon electrochemical reduction, with ∼80% of the products **2a** and **3a** formed. Then **2a** was further reduced over the course of the remaining 2.5 h, ultimately converted to **4a**. This experiment indicates that the pinacol product **4a** is the result of a second reduction of aromatic ketone **2a**.

During optimization, we discovered that electrolyte identity impacted product isolation. Large concentrations of highly soluble tetraalkylammonium salts, such as NBu_4ClO_4 and NBu_4PF_6, are difficult to remove from the crude reaction mixture by column chromatography. Extraction was also attempted but failed to recover products in high yields due to moderate solubility of **2a** and **3a** in aqueous solutions. This electrochemical reduction requires an inexpensive electrolyte that satisfies the following three criteria. First, the electrolyte must have a wide background potential, beyond the range of −3.0 V on the reduction side, available for the ketone reduction. Second, the electrolyte must be highly solubilized and ionized in polar solvent like MeCN to provide a conductive atmosphere for electron flow. Third, the electrolyte must be easily removable from the reaction to afford pure products.

Metal salts were first attempted to use as alternative electrolytes for more facile separation. However, when $NaClO_4$ was used, the reaction current dropped to zero within 30 min, and only ∼10% of **1a** was converted, with <10% formation of **2a** (Figure 3A, entry 2). The phenol fragment **3a** was not detected throughout the reaction. Instead, a white solid coated on the electrode surface was observed and characterized as sodium phenoxide salt **3a′** by NMR; i.e., the

https://doi.org/10.1021/acs.joc.1c00346
J. Org. Chem. XXXX, XXX, XXX−XXX

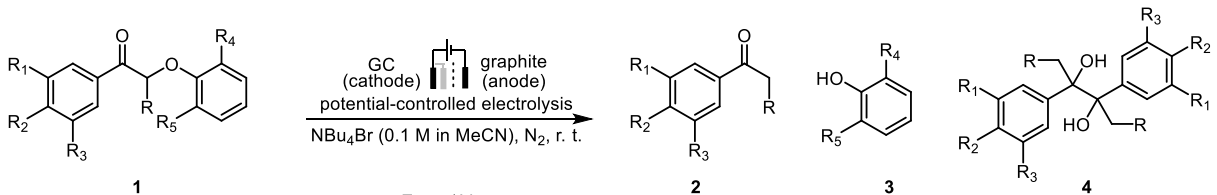

1 2 3 4

Substrate 1							E_{apply} / V vs Fc^+/Fc	time	isolated yields		
	R	R_1	R_2	R_3	R_4	R_5					
1a	H	H	OMe	H	OMe	H	-2.3 V	4 h	**2a** 86% (84%)[a] (72%)[b]	**3a** 92% (75%)[a] (65%)[b]	
							-2.7 V	6 h		**3a** 86%	**4a** 75%
1b	H	OMe	OMe	H	OMe	H	-2.3 V	4 h	**2b** 86%	**3a** 86%	
							-2.7 V	6 h		**3a** 86%	**4b** 86%
1c	H	OMe	OMe	OMe	OMe	H	-2.3 V	4 h	**2c** 81%	**3a** 92%	
							-2.7 V	6 h		**3a** 82%	**4c** 68%
1d	CH_2OH	H	OMe	H	OMe	H	-2.3 V [c]	4 h	**2d** 82%	**3a** 72%	
							-2.7 V [d]	6 h		**3a** 72%	**4d** 84%
1e	CH_2OH	OMe	OMe	H	OMe	OMe	-2.3 V [c]	4 h	**2e** 85%	**3b** 78%	
							-2.7 V [d]	6 h		**3b** 74%	**4e** 86%
1f	CH_2OH	OMe	OMe	OMe	OMe	H	-2.3 V [c]	4 h	**2f** 74%	**3a** 75%	
							-2.7 V [d]	6 h		**3a** 72%	**4f** 69%
1h	H	H	OH	H	OMe	H	-2.0 V [e]	4 h	**2h** 59%	**3a** 75%	

Figure 4. Electrochemical reduction of oxidized lignin model substrates. Conditions: **1** (0.16 mmol, 20 mM), NBu_4Br (0.1 M in 8 mL MeCN), N_2 protection, glassy carbon cathode, graphite anode, $Ag/AgNO_3$ reference electrode, divided cell, constant potential control. Products were purified by column chromatography, and isolated yields were reported. (a) Undivided cell electrolysis. (b) One-gram scale electrolysis, 48 h. (c) Addition of AcOH (5 equiv). (d) Addition of AcOH (8 equiv). (e) MeCN/DMF (v/v 7:1) as solvent.

precipitation of insoluble metal salt deactivated the electrode surface. We also encountered this problem when performing multiple-cycle cyclic voltammetry experiments. Unlike NBu_4ClO_4, reduction of **1a** occurred at a more positive potential when $NaClO_4$ was used in the electrolyte. Additionally, the current decreased over multiple cycles due to precipitation of sodium phenoxide (Figure 3C, top). A relevant electrolyte screening suggested that this problem was widespread among most common metal cations, such as lithium, sodium, potassium, and magnesium (SI). Upon evaluation of a variety of salts, tetrabutylammonium bromide (NBu_4Br) was chosen as electrolyte. NBu_4Br provides a conductive reaction media with a wide potential window up to −3.0 V, resulting in high isolated yields (86% of **2a** and 92% of **3a**, Figure 3A, entry 4). After the reaction, NBu_4Br can be easily removed by column chromatography. Furthermore, from a safety perspective, NBu_4Br is easier to operate on a large scale in comparison to perchlorate salts.

Compared to our previous method utilizing photochemical lignin fragmentation, acid was not explicitly added even though the reductions involved a proton/hydrogen transfer. Taking all possibilities into consideration, the proton/hydrogen could come from either one of two possible sources, the background salt (NBu_4Br) or the solvent (MeCN). A series of control experiments was conducted to distinguish these possibilities. First, a poor proton/hydrogen donor bis(triphenylphosphoranylidene)ammonium chloride (PPNCl) was used as the background salt for comparison with tetraalkylammonium salts (voltammetry in SI). Electrolysis of **1a** with PPNCl gave nearly full conversion, providing evidence against tetrabutylammonium cations as a necessary proton/hydrogen source (Figure 3A, entry 5). Second, an isotope labeling experiment was performed. Lignin model **1a** was first considered as the model substrate; however, electrolysis of **1a** within a solution of NBu_4Br in deuterium acetonitrile (MeCN-d_3) did not yield any desired products. The results can be explained by a competing reaction that converts intermediate $\mathbf{1a}^{\bullet-}$ to other products. The existence of other competing reactions was also supported by cyclic voltammetry (SI). In the presence of MeCN-d_3, the current magnitude of the second reduction peak decreased by 32%. Performing the same measurements at a slower scan rate (decreasing from 0.1 to 0.01 V s^{-1}) resulted in a larger decrease of 36%; i.e., less **2a** was formed at a longer time scale experiment due to a side reaction. Then substrate **1g** bearing a *gem*-dimethyl group on the C_β position was used to conduct similar experiments. In MeCN-d_3, deuterium-labeled aromatic ketone **2g** (>95% atom D by ^1H NMR) was isolated in 70% yield, indicating the role of MeCN as the proton/hydrogen donor (Figure 3B). Different from **1a**, the second reduction peak showed more similarity in magnitude between MeCN and MeCN-d_3 at a slower scan rate (22% decrease) in comparison with that at a higher scan rate (28% decrease) (SI). Possibly, **1g** forms a more stable intermediate and a slower competing reaction is balanced out by the kinetic isotope effect. Taking all the information together, the results demonstrate that MeCN is a proton/hydrogen donor. Aforementioned path a is the major but probably not only mechanism. Furthermore, the selection of proton/hydrogen donor is critical to achieve high yields.

The applicability of the electrochemical reduction approach was then examined on other β-O-4 models. Adding methoxy groups at C_3 and C_5 gave coniferyl alcohol derived model **1b** and sinapyl alcohol derived model **1c**, respectively. Their redox responses featured two subsequent reduction peaks, with the

https://doi.org/10.1021/acs.joc.1c00346
J. Org. Chem. XXXX, XXX, XXX−XXX

second peak corresponding to the reduction of their corresponding fragmentation products **2b** and **2c**, which were similar to **1a**. Subjecting **1b** and **1c** to the optimized conditions delivered fragmentation and/or coupling products in isolated yields of 68−92% (Figure 4).

Next, substrate **1d** bearing the hydroxymethyl group on the C_β position was tested. The redox response for reduction of **1d** exhibited different characteristics from **1a**−**1c** (SI). Near −2.7 V, multiple redox waves were visible rather than just one wave as in Figure 2B. At least three distinct redox signatures were evident. In addition, the overall peak occurred at −0.1 V more negative than the reduction of the corresponding fragmentation product **2d**. These observations suggested a more complicated reduction mechanism. Indeed, electrolysis of **1d** at peak potentials E_{p1} or E_{p2} gave **3a** in ∼70% isolated yields but failed in producing any aromatic ketone product **2d**. Substrate **1d** decomposed to a mixture of higher molecule weight trimers, presumably from a competing reaction due to lack of effective proton/hydrogen donors for this type of model substrate. Thus, acetic acid (AcOH, 5 equiv) was added as a proton source. At −2.3 V, the desired products **2d** and **3a** were isolated in 82% and 72% yield, respectively. Notably, reduction of **1d** and **2d** both occurred at slightly more positive potentials due to carbonyl activation under acidic conditions (SI). In the presence of acetic acid, those two reduction reactions are both spontaneous at −2.3 V, but reduction of **1d** is thermodynamically preferred, leading to selective formation of **2d** as the major product. Applying a more negative potential of −2.7 V delivered products **2d** and **3a** with the addition of AcOH (8 equiv) and gave 71% and 84% isolated yields, respectively. Similarly, electrolyzing **1e** and **1f** with acetic acid as a proton donor additive gave the desired products in isolated yields of 69% to 86%.

Finally, the possibility of reacting native lignin instead of lignin models was evaluated. First, considering a 4-hydroxylacetophenone-type molecule will be the major product from lignin degradation, a phenolic lignin model **1h** was subjected to the optimized conditions and gave **2h** and **3a** in 59% and 75% isolated yields, respectively. Second, electrolysis of **1a** was performed in an undivided cell to simplify the reaction setup and resulted in **2a** (84%) and **3a** (75%) with a minimal yield decrease. Third, a gram-scale electrolysis of **1a** was conducted to demonstrate reaction scalability, with reasonable isolated yields of **2a** (72%) and **3a** (65%). Despite the promising results presented herein, a few challenges to realize an optimal and technologically viable lignin electro-degradation still exist. First, native lignin is highly insoluble in organic solvents, and thus development of a method for soluble lignin separation is still necessary. Second, a large amount of different products may cause an isolation issue, and the development of highly selective degradation method is critical. Third, lignin processing is anticipated to operate on an immense scale, and the application of continuous flow technology to these reactions should be pursued. This study focuses on the fundamental aspects of reaction reactivity and selectivity and hopefully stimulate future work in this area.

CONCLUSIONS

In summary, this paper details an electro-reductive method for lignin degradation. Potential-controlled electrolyses provide fragmentation and coupling products in high selectivity and isolated yields of 59−92%. The condition optimization and mechanistic details speak to the critical roles of background salts and solvent in this transformation, providing a good template for condition selections. The same principles can apply to reaction conditions germane to native lignin. We anticipate the incorporation of electrochemistry and principles for lignin valorization to be of great value to a greener chemical production process and a sustainable future.

EXPERIMENTAL SECTION

General Information. Thin-layer chromatography (TLC) was performed on Merck silica gel 60 F254 TLC plates, visualized by a dual short wave/long wave UV lamp and stained using *p*-anisaldehyde. Column chromatography was performed manually using 43−60 μm (230−400 mesh) silica gel. Commercially available chemicals were used as received without purifications. All electrolytes were electrochemical-grade chemicals. Substrates **1a**−**1g** were prepared according to the reported procedures.[24−26] Products **2a**−**2f** and **3a**,**b** were previously reported compounds.[13,24]

Cyclic voltammetry measurements were performed with a CHI 620E Potentiostat (purchased from CH Instrument) in a voltammetry cell SVC-3 (purchased from Bio-Logic) utilizing a three-electrode setup consisting of glassy carbon working electrode (3 mm diameter, purchased from CH Instrument), a graphite counter electrode (purchased from McMASTER-CARR), and a handmade Ag/$AgNO_3$ (0.01 M $AgNO_3$, 0.1 M NBu_4ClO_4 in MeCN) reference electrode. The glassy carbon electrode was polished with 5, 1, and 0.05 μm alumina slurries and dried by blowing nitrogen before each experiment. All reported potentials were calibrated by ferrocenium/ferrocene (Fc^+/Fc) after each experiment.

Bulk electrolysis experiments were performed with a CHI 620E potentiostat (purchased from CH Instrument) or μStat 4000 multichannel potentiostat/galvanostat (purchased from Metrohm USA) and in a divided electrochemical cell made by the Glass Blowing Office at the Department of Chemistry, University of Michigan, Ann Arbor, MI. A frit disk with porosity of 5 (no. 15105, purchased from ROBU) was used to separate the anodic and cathodic chambers. (Note: The highest operating temperature of this frit is 80 °C. The divided cell was rinsed with clean solvents and dried under N_2 without any heat after each experiment.) For small-scale reaction, a glassy carbon plate (No. 613-422-20, purchased from Goodfellow) was used as a cathode (working electrode), and a graphite rod was used as an anode. For a gram-scale reaction, reticulated vitreous carbon foam (RVC, No. 613-422-20, purchased from Goodfellow) was used as cathode and anode. A handmade Ag/$AgNO_3$ (0.01 M $AgNO_3$, 0.1 M NBu_4ClO_4 in MeCN) electrode was used as a reference. All applied potentials were reported with respect to the standard potential of ferrocenium/ferrocene $E^{0\prime}$(Fc^+/Fc).

Gas chromatography−mass spectrometry (GC−MS) analysis was performed on a Shimadzu QP-2010, with an electron impact ion source. Nuclear magnetic resonance (NMR) spectra were recorded using an internal deuterium lock on Varian MR500 and Varian Inova 500 spectrometers at the Department of Chemistry instrumentation facility, University of Michigan, Ann Arbor, MI. Chemical shifts (δ) are reported in parts per million (ppm), and are quoted to two decimal places and a single decimal place for ^{1}H and ^{13}C NMR, respectively, with coupling constants (J) expressed in hertz (Hz) to the nearest 0.1 Hz. The chemical shifts are reported relative to the deuterated solvent resonance ($CDCl_3$: δ H = 7.26 ppm and δ C = 77.2 ppm; MeCN-d_3: δ H = 1.94 ppm and δ C = 118.3 ppm; D_2O: δ H = 4.79 ppm). Multiplicities are reported using the following abbreviations: s = singlet, d = doublet, t = triplet, m = multiplet, br s = broad singlet, dd = doublet of doublet etc. High-resolution mass spectra (HRMS) were obtained on a Micromass AutoSpec Ultima Magnetic Sector mass spectrometer using electrospray ionization (ESI), positive-ion mode on an Agilent Q-TOF (model G6520B) HPLC-MS system, at the Department of Chemistry instrumentation facility, University of Michigan, Ann Arbor, MI.

Procedure for Electrochemical Reduction of 1a Using Constant Current Method. The reaction was performed in a divided cell equipped with a glassy carbon plate cathode (2 cm^2), a

https://doi.org/10.1021/acs.joc.1c00346
J. Org. Chem. XXXX, XXX, XXX−XXX

graphite anode. A solution of 0.1 M NBu_4ClO_4 in MeCN was used as a conductive reaction media. To the cathodic chamber were added **1a** (0.16 mmol, 1 equiv) and 8 mL of electrolyte solution. To the anodic chamber, 2 mL of electrolyte solution was added. The reaction was performed under the protection of nitrogen at room temperature with a constant current of 3.3 mA for 4 h (~3 equiv of electrons). After the reaction was completed, solvent was removed under reduced pressure and the resulting crude mixture was analyzed by ^{1}H NMR using 1,3,5-trimethoxybenzene as an internal standard. The reaction gave ~43% ^{1}H NMR yield of **2a**, ~86% ^{1}H NMR yield of **3a**, and ~41% ^{1}H NMR yield of **4a**. The structure of **4a** was determined by comparison to a previous report.[27] (Note: Due to a large amount of electrolyte in the crude mixture, the signals in ^{1}H NMR were distorted to some extent and the reported yields here were rough estimations.)

General Procedure for Reaction Optimization. Reaction was performed in a divided cell equipped with a glassy carbon plate cathode (2 cm^2), a graphite anode, and a $Ag/AgNO_3$ reference electrode. A solution of 0.1 M electrolyte in MeCN was used as a conductive medium. To the cathodic chamber were added **1a** (0.16 mmol, 1 equiv) and 8 mL of electrolyte solution. To the anodic chamber, 2 mL of reaction solution was added. Bulk electrolysis was performed under the protection of nitrogen at room temperature with a constant potential. After the reaction was completed, solvent was removed under reduced pressure and the resulting crude mixture was analyzed by ^{1}H NMR using 1,3,5-trimethoxybenzene as an internal standard. A full optimization table is presented in the SI.

Monitoring the Reaction Progress by GCMS. Electrolysis of **1a** was performed with NBu_4ClO_4 at a constant potential of −2.7 V for 6 h. An aliquot reaction solution was taken for GC−MS analysis every 30 min and was reinjected into reaction solution. The concentrations for each molecule were calculated according to their premade calibration curves. Tabulated raw data is presented in the SI.

*Sodium 2-Methoxyphenoxide (**3a′**).* White solid. Yield: 4 mg (<10%), from electrolysis of **1a** with $NaClO_4$. After the reaction, a white solid coated on the cathode was isolated. The solid was rinsed with MeCN (3 mL × 3) and dried over vacuum. The major species in the crude solid was characterized as **3a′**. ^{1}H NMR (500 MHz, D_2O) δ: 6.90 (dd, 1H, J = 7.9, 1.4 Hz), 6.83−6.79 (dt, 1H, J = 7.8, 1.5 Hz), 6.67−6.65 (dd, 1H, J = 7.8, 1.5 Hz), 6.59−6.55 (dt, 1H, J = 7.8, 1.5 Hz), 3.75 (s, 3H). ^{13}C{^{1}H} NMR (126 MHz, $CDCl_3$) δ: 161.0, 147.9, 121.7, 119.8, 116.1, 112.8, 55.9.

General Procedure for Electrochemical Reductive Cleavage of Substrates 1a−1g. The reaction was performed in a divided cell equipped with a glassy carbon plate cathode (2 cm^2), a graphite anode and a $Ag/AgNO_3$ reference electrode. A solution of 0.1 M NBu_4Br in MeCN was used as a conductive reaction media. To the cathodic chamber were added **1** (0.16 mmol, 1 equiv) and 8 mL of electrolyte solution. To the anodic chamber was added 2 mL of electrolyte solution. Bulk electrolysis was performed under the protection of nitrogen at room temperature with a constant potential. After the reaction was completed, solvent was removed under reduced pressure. The corresponding products **2**−**4** were purified by column chromatography on silica gel using ethyl acetate/hexanes.

Reaction of **1a** (44 mg) at −2.3 V for 4 h produced **2a** (21 mg, 86% yield) and **3a** (18 mg, 92%). *1-(4-methoxyphenyl)ethan-1-one* (**2a**).[13,24] Colorless, amorphous solid. ^{1}H NMR (500 MHz, $CDCl_3$) δ: 7.92 (d, 2H, J = 8.9 Hz), 6.92 (d, 2H, J = 8.8 Hz), 3.85 (s, 3H), 2.54 (s, 3H). ^{13}C{^{1}H} NMR (126 MHz, $CDCl_3$) δ: 196.7, 163.4, 130.5, 130.2, 113.6, 55.5, 26.4. *2-Methoxyphenol* (**3a**).[13,24] Colorless oil. ^{1}H NMR (500 MHz, $CDCl_3$) δ: 6.96−6.94 (m, 1H), 6.90−6.85 (m, 3H), 5.66 (br s, 1H), 3.89 (s, 3H). ^{13}C{^{1}H} NMR (126 MHz, $CDCl_3$) δ: 146.8, 145.8, 121.5, 120.2, 114.8, 111.0, 55.9. Purified by gradient elution (10−40% ethyl acetate/hexanes) column chromatography on silica gel.

Reaction of **1b** (48 mg) at −2.3 V for 4 h produced **2b** (23 mg, 86% yield) and **3a** (17 mg, 86%). *1-(3,4-dimethoxyphenyl)ethan-1-one* (**2b**).[13,24] Colorless, amorphous solid. ^{1}H NMR (500 MHz, $CDCl_3$) δ: 7.55 (dd, 1H, J = 8.4, 2.1 Hz), 7.51 (m, 1H), 6.87 (d, 1H, J = 8.4 Hz), 3.93 (s, 3H), 3.92 (s, 3H), 2.55 (s, 3H). ^{13}C{^{1}H} NMR (126 MHz, $CDCl_3$) δ: 196.6, 153.1, 148.7, 130.2, 123.0, 109.7, 55.8, 26.1. Purified by gradient elution (10−40% ethyl acetate/hexanes) column chromatography on silica gel.

Reaction of **1c** (53 mg) at −2.3 V for 4 h produced **2c** (27 mg, 81%) and **3a** (18 mg, 92%). *1-(3,4,5-trimethoxyphenyl)ethan-1-one* (**2c**).[13,24] Colorless, amorphous solid. Yield: from electrolysis of **1c** at −2.3 V for 4 h. ^{1}H NMR (500 MHz, $CDCl_3$) δ: 7.22 (s, 2H), 3.92 (s, 6H), 3.92 (s, 3H), 2.59 (s, 3H). ^{13}C{^{1}H} NMR (126 MHz, $CDCl_3$) δ: 196.8, 153.0, 142.5, 132.4, 105.6, 60.8, 56.1, 26. 5. Purified by gradient elution (10−40% ethyl acetate/hexanes) column chromatography on silica gel.

Reaction of **1d** (48 mg) at −2.3 V for 4 h, with addition of AcOH (0.8 mmol, 5 equiv) to the cathodic chamber, produced **2d** (24 mg, 82%) and **3a** (13 mg, 72%). *3-Hydroxy-1-(4-methoxyphenyl)propan-1-one* (**2d**).[13,24] Colorless, amorphous solid. ^{1}H NMR (500 MHz, $CDCl_3$) δ: 7.94 (d, 2H, J = 8.9 Hz), 6.94 (d, 2H, J = 8.9 Hz), 4.01 (q, 2H, J = 11.2, 5.6 Hz), 3.88 (s, 3H), 3.18 (t, 2H, J = 5.4 Hz), 2.76 (m, 1H). ^{13}C{^{1}H} NMR (126 MHz, $CDCl_3$) δ: 199.2, 164.0, 130.5, 114.0, 58.4, 55.7, 40.2. Purified by gradient elution (10−50% ethyl acetate/hexanes) column chromatography on silica gel.

Reaction of **1e** (58 mg) at −2.3 V for 4 h, with addition of AcOH (0.8 mmol, 5 equiv) to the cathodic chamber, produced **2e** (29 mg, 85%) and **3b** (19 mg, 78%). *1-(3,4-Dimethoxyphenyl)-3-hydroxypropan-1-one* (**2e**).[13,24] Colorless, amorphous solid. ^{1}H NMR (500 MHz, $CDCl_3$) δ: 7.59 (dd, 1H, J = 8.3, 2.0 Hz), 7.52 (s, 1H), 6.90 (d, 1H, J = 8.4 Hz), 4.02 (q, 2H, J = 11.9, 5.2 Hz), 3.95 (s, 3H), 3.94 (s, 3H), 3.19 (t, 2H, J = 5.4 Hz), 2.73 (t, 1H, J = 6.6 Hz). ^{13}C{^{1}H} NMR (126 MHz, $CDCl_3$) δ: 198.06, 152.6, 148.0, 128.9, 121.9, 109.0, 108.8, 57.3, 55.1, 55.0, 38.8. *2,6-Dimethoxyphenol* (**3b**).[13,24] Colorless, amorphous solid. ^{1}H NMR (500 MHz, $CDCl_3$) δ: 6.79 (t, 1H, J = 8.6 Hz,), 6.59 (s, 1H), 6.58 (s, 1H), 5.51 (br s, 1H), 3.89 (s, 6H); ^{13}C{^{1}H} NMR (126 MHz, $CDCl_3$) δ: 147.3, 134.9, 119.1, 105.0, 56.3. Purified by gradient elution (10−50% ethyl acetate/hexanes) column chromatography on silica gel.

Reaction of **1f** (58 mg) at −2.3 V for 4 h, with addition of AcOH (0.8 mmol, 5 equiv) to the cathodic chamber, produced **2f** (28 mg, 74%) and **3a** (14 mg, 75%). *3-Hydroxy-1-(3,4,5-trimethoxyphenyl)-propan-1-one* (**2f**).[13,24] Colorless, amorphous solid. Yield: 28 mg (74%), from electrolysis of **1f** at −2.3 V for 4 h, with addition of AcOH (0.8 mmol, 5 equiv) to the cathodic chamber. ^{1}H NMR (500 MHz, $CDCl_3$) δ: 7.23 (s, 2H), 4.3 (q, 2H, J = 11.5, 5.7 Hz), 3.93 (s, 9H), 3.21 (t, 2H, J = 5.3 Hz), 2.61 (t, 1H, J = 6.7 Hz). ^{13}C{^{1}H} NMR (126 MHz, $CDCl_3$) δ: 199.2, 153.1, 143.0, 131.9, 105.6, 61.0, 58.2, 56.3, 40.1. Purified by gradient elution (10−50% ethyl acetate/hexanes) column chromatography on silica gel.

Reaction of **1g** (48 mg) at −2.3 V for 4 h in MeCN-d_3 produced **2g** (20 mg, 70% yield) and **3a** (12 mg, 64%). *1-(4-Methoxyphenyl)-2-methylpropan-1-one-2-d* (**2g**). Colorless, amorphous solid, > 95% atom D. ^{1}H NMR (500 MHz, $CDCl_3$) δ: 7.96−7.94 (d, 2H, J = 8.9 Hz), 6.93−6.95 (d, 2H, J = 8.8 Hz), 3.87 (s, 3H), 1.20 (s, 3H). ^{13}C{^{1}H} NMR (126 MHz, $CDCl_3$) δ: 203.11, 163.3, 130.5, 129.2, 113.7, 55.5, 19.2; HRMS (ESI/Q-TOF) m/z: $[M + H]^+$ Calcd for $C_{11}H_{14}DO_2^+$ 180.1129; Found: 180.1117. Purified by gradient elution (10−40% ethyl acetate/hexanes) column chromatography on silica gel.

Reaction of **1a** (44 mg) at −2.7 V for 6 h produced **4a** (36 mg, 75%, *meso*/*dl* = 44:56) and **3a** (17 mg, 86%). *2,3-Bis(4-methoxyphenyl)butane-2,3-diol* (**4a**). Colorless, amorphous solid. *meso* isomer: ^{1}H NMR (500 MHz, $CDCl_3$) δ: 7.32−7.10 (m, 4H), 6.89−6.76 (m, 4H), 3.80 (s, 6H), 2.21 (br s, 2H), 1.56 (s, 3H). ^{13}C{^{1}H} NMR (126 MHz, $CDCl_3$) δ: 158.4, 135.7, 128.1, 112.4, 78.5, 55.2, 25.0. *dl* isomer: ^{1}H NMR (500 MHz, $CDCl_3$) δ: 7.32−7.10 (m, 4H), 6.89−6.76 (m, 4H), 3.81 (s, 6H), 2.48 (br s, 2H), 1.47 (s, 3H). ^{13}C{^{1}H} NMR (126 MHz, $CDCl_3$) δ: 158.5, 136.0, 128.5, 112.5, 78.7, 55.2, 25.2. HRMS (ESI/Q-TOF) m/z: $[M + Na]^+$ Calcd for $C_{18}H_{22}NaO_4^+$ 325.1416; Found: 325.1409. Purified by gradient elution (10−70% ethyl acetate/hexanes) column chromatography on silica gel.

Reaction of **1b** (48 mg) at −2.7 V for 6 h produced **4b** (42 mg, 72%, *meso*/*dl* = 51:49) and **3a** (17 mg, 86%). *2,3-Bis(3,4-dimethoxyphenyl)butane-2,3-diol* (**4b**). Yellow, amorphous solid. *Meso* isomer: ^{1}H NMR (500 MHz, $CDCl_3$) δ: 6.95−6.95 (m, 2H), 6.90−

https://doi.org/10.1021/acs.joc.1c00346
J. Org. Chem. XXXX, XXX, XXX−XXX

6.88 (m, 2H), 6.84−6.83 (m, 2H), 4.86 (q, 1H, J = 10.0, 5.0 Hz), 3.90 (s, 3H), 3.87 (s, 6H), 1.50 (s, 6H). $^{13}C\{^1H\}$ NMR (126 MHz, $CDCl_3$) δ: 148.0, 132.5, 121.0, 112.0, 109.7, 82.4, 60.3, 55.8, 55.8, 35.1. *dl* isomer: ^1H NMR (500 MHz, $CDCl_3$) δ: 6.95−6.95 (m, 2H), 6.90−6.88 (m, 2H), 6.84−6.83 (m, 2H), 4.86 (q, 2H, J = 10.0, 5.0 Hz), 3.90 (s, 3H), 3.87 (s, 3H), 1.48 (s, 6H). $^{13}C\{^1H\}$ NMR (126 MHz, $CDCl_3$) δ: 148.0, 132.5, 121.0, 112.0, 109.7, 82.4, 60.3, 55.8, 55.8, 35.1. HRMS (ESI/Q-TOF) m/z: $[M + NH_4]^+$ Calcd for $C_{20}H_{30}NO_6^+$ 380.2073; Found 380.2063. Purified by gradient elution (10−70% ethyl acetate/hexanes) column chromatography on silica gel.

Reaction of **1c** (53 mg) at −2.7 V for 6 h produced **4c** 46 mg (68%, *meso*/*dl* = 50:50) and **3a** (16 mg, 82%). *2,3-Bis(3,4,5-trimethoxyphenyl)butane-2,3-diol* (**4c**). Yellow, amorphous solid. *Meso* isomer: ^1H NMR (500 MHz, $CDCl_3$) δ: 6.60 (s, 4H), 4.87−4.82 (m, 2H), 3.87 (s, 12H), 3.83 (s, 6H), 1.50 (s, 3H). $^{13}C\{^1H\}$ NMR (126 MHz, $CDCl_3$) δ: 153.3, 141.7, 137.1, 102.2, 70.6, 60.8, 56.1, 25.2. *dl* isomer: ^1H NMR (500 MHz, $CDCl_3$) δ: 6.60 (s, 4H), 4.87−4.82 (m, 2H), 3.87 (s, 12H), 3.83 (s, 6H), 1.49 (s, 6H). $^{13}C\{^1H\}$ NMR (126 MHz, $CDCl_3$) δ: 153.3, 141.7, 137.1, 102.2, 70.6, 60.8, 56.1, 25.2. HRMS (ESI/Q-TOF) m/z: $[M + NH_4]^+$ Calcd for $C_{22}H_{34}NO_8^+$ 440.2284; Found 440.2279. Purified by gradient elution (10−70% ethyl acetate/hexanes) column chromatography on silica gel.

Reaction of **1d** (48 mg) at −2.7 V for 6 h, with addition of AcOH (1.28 mmol, 8 equiv) to the cathodic chamber, produced **4d** (49 mg (84%, *meso*/*dl* = 54:46) and **3a** (13 mg, 72%). *3,4-Bis(4-methoxyphenyl)hexane-1,3,4,6-tetraol* (**4d**). Colorless, amorphous solid. *meso* isomer: ^1H NMR (500 MHz, MeCN-d_3) δ: 7.04−6.76 (m, 8H), 4.68 (s, 2H), 3.76 (s, 6H), 3.42−3.32 (m, 4H), 2.93 (s, 2H), 2.32−2.26 (m, 2H), 1.78−1.75 (m, 2H). $^{13}C\{^1H\}$ NMR (126 MHz, MeCN-d_3) δ: 159.4, 134.3, 130.4, 113.0, 82.4, 60.1, 55.7, 36.4. *dl* isomer: ^1H NMR (500 MHz, MeCN-d_3) δ: 7.04−6.76 (m, 8H), 4.68 (s, 2H), 3.76 (s, 6H), 3.42−3.32 (m, 4H), 2.93 (s, 2H), 2.32−2.26 (m, 2H), 1.74−1.73 (m, 2H). $^{13}C\{^1H\}$ NMR (126 MHz, MeCN-d_3) δ: 159.4, 134.3, 130.4, 113.0, 82.4, 60.1, 55.7, 36.4. HRMS (ESI/Q-TOF) m/z: $[M + Na]^+$ Calcd for $C_{20}H_{26}NaO_6^+$ 385.1627; Found 385.1622. Purified by gradient elution (10−70% ethyl acetate/hexanes) column chromatography on silica gel.

Reaction of **1e** (58 mg) at −2.7 V for 6 h, with addition of AcOH (1.28 mmol, 8 equiv) to the cathodic chamber, produced **4e** 58 mg (86%, *meso*/*dl* = 63:37) and **3b** (18 mg, 74%). *3,4-Bis(3,4-dimethoxyphenyl)hexane-1,3,4,6-tetraol* (**4e**). Yellow, amorphous solid. *Meso* isomer: ^1H NMR (500 MHz, $CDCl_3$) δ: 6.94−6.83 (m, 6H), 4.93−4.91 (m, 2H), 3.90−3.88 (m, 12H), 3.88−3.73 (m, 4H), 2.69 (br s, 1H), 2.31 (br s, 1H), 2.05−2.00 (m, 2H), 1.94−1.93 (m, 2H). $^{13}C\{^1H\}$ NMR (126 MHz, $CDCl_3$) δ: 148.0, 132.5, 121.0, 112.0, 109.7, 82.4, 60.3, 55.8, 55.8, 35.1. *dl* isomer: ^1H NMR (500 MHz, $CDCl_3$) δ: 6.94−6.83 (m, 6H), 4.93−4.91 (m, 2H), 3.90−3.88 (m, 12H), 3.88−3.73 (m, 4H), 2.69 (br s, 1H), 2.31 (br s, 1H), 2.08−2.03 (m, 2H), 1.93−1.90 (m, 2H). $^{13}C\{^1H\}$ NMR (126 MHz, $CDCl_3$) δ: 148.0, 132.5, 121.0, 112.0, 109.9, 82.4, 60.6, 55.8, 55.8, 36.0. HRMS (ESI/Q-TOF) m/z: $[M + Na]^+$ Calcd for $C_{22}H_{30}NaO_8^+$ 445.1838; Found 445.1833. Purified by gradient elution (10−70% ethyl acetate/hexanes) column chromatography on silica gel.

Reaction of **1f** (58 mg) at −2.7 V for 6 h, with addition of AcOH (1.28 mmol, 8 equiv) to the cathodic chamber, produced **4f** 53 mg (69%, *meso*/*dl* = 69:31) and **3a** (13 mg, 72%). *3,4-Bis(3,4,5-trimethoxyphenyl)hexane-1,3,4,6-tetraol* (**4f**). Yellow, amorphous solid. *Meso* isomer: ^1H NMR (500 MHz, $CDCl_3$) δ: 6.60 (s, 2H), 4.90 (m, 2H), 3.92−3.89 (m, 4H), 3.87 (s, 12H), 3.83 (s, 6H), 2.86 (br s, 1H), 2.29 (br s, 1H), 2.03−1.98 (m, 2H), 1.95−1.92 (m, 2H). $^{13}C\{^1H\}$ NMR (126 MHz, $CDCl_3$) δ: 153.6, 140.5, 137.5, 102.8, 74.9, 61.9, 61.2, 56.4, 40.9. *dl* isomer: ^1H NMR (500 MHz, $CDCl_3$) δ: 6.60 (s, 2H), 4.90 (m, 2H), 3.92−3.89 (m, 4H), 3.87 (s, 12H), 3.83 (s, 6H), 2.86 (br s, 1H), 2.29 (br s, 1H), 2.06−2.01 (m, 2H), 1.93−1.90 (m, 2H). $^{13}C\{^1H\}$ NMR (126 MHz, $CDCl_3$) δ: 153.6, 140.5, 137.5, 102.8, 74.9, 61.9, 61.2, 56.4, 40.9. HRMS (ESI/Q-TOF) m/z: $[M + Na]^+$ Calcd for $C_{24}H_{34}NaO_{10}^+$ 505.2050; Found 505.2044. Purified by gradient elution (10−70% ethyl acetate/hexanes) column chromatography on silica gel.

Electrochemical Reductive Cleavage of Substrate 1h. Reaction was performed in a divided cell equipped with a glassy carbon plate cathode (2 cm^2), a graphite anode, and a $Ag/AgNO_3$ reference electrode. A solution of 0.1 M NBu_4Br in MeCN/DMF (v:v 7:1) was used as a conductive reaction media. DMF was used to solubilize polar substrate **1h**. To the cathodic chamber were added **1h** (41 mg, 0.16 mmol, 1 equiv) and 8 mL of electrolyte solution. To the anodic chamber was added 2 mL of electrolyte solution. Bulk electrolysis was performed under the protection of nitrogen at room temperature with a constant potential of −2 V for 4 h. After the reaction was completed, solvent was removed under reduced pressure. The crude mixture was purified by column chromatography on silica gel using gradient elution (10−80% ethyl acetate/hexanes) and gave the corresponding products **2h** (13 mg, 59%) and **3a** (14 mg, 75%). *1-(4-Hydroxyphenyl)ethan-1-one* (**2h**).[26] Colorless, amorphous solid. ^1H NMR (500 MHz, $CDCl_3$) δ: 7.92 (d, 2H, J = 8.8 Hz), 6.94 (d, 2H, J = 8.8 Hz), 7.17 (br s, 1H), 2.58 (s, 3H), $^{13}C\{^1H\}$ NMR (126 MHz, $CDCl_3$) δ: 198.2, 161.0, 131.2, 129.8, 115.5, 26.31.

Undivided Cell Electrolysis of 1a. The reaction was performed in an undivided cell equipped with a glassy carbon plate cathode (2 cm^2), a graphite anode, and a $Ag/AgNO_3$ reference electrode. A solution of 0.1 M NBu_4Br in MeCN was used as a conductive reaction media. To the cell were added **1a** (44 mg, 0.16 mmol, 1 equiv) and 8 mL of electrolyte solution. Bulk electrolysis was performed under the protection of nitrogen at room temperature with a constant potential of −2.2 V for 4 h. After the reaction was completed, solvent was removed under reduced pressure. The crude mixture was purified by column chromatography on silica gel using gradient elution (10−40% ethyl acetate/hexanes) and gave the corresponding products **2a** (20 mg, 84%) and **3a** (14 mg, 75%).

Gram-Scale Electrolysis of 1a. The reaction was performed in a divided cell equipped with an RVC cathode, an RVC anode, and a $Ag/AgNO_3$ reference electrode. A solution of 0.1 M NBu_4Br in MeCN was used as a conductive reaction medium. To the cathodic chamber were added **1a** (1 g, 3.7 mmol) and 185 mL of electrolyte solution. To the anodic chamber was added 185 mL of electrolyte solution. Bulk electrolysis was performed under the protection of nitrogen at room temperature with a constant potential of −2.2 V for 48 h. After the reaction was completed, solvent was removed under reduced pressure. The crude mixture was purified by column chromatography on silica gel using gradient elution (10−40% ethyl acetate/hexanes) and gave the corresponding products **2a** (0.4 g, 72%) and **3a** (0.3 g, 65%).

■ ASSOCIATED CONTENT

Supporting Information

The Supporting Information is available free of charge at https://pubs.acs.org/doi/10.1021/acs.joc.1c00346.

Additional experimental data, cyclic voltammograms and NMR spectra (PDF)

■ AUTHOR INFORMATION

Corresponding Author

Corey R. J. Stephenson − *Willard Henry Dow Laboratory, Department of Chemistry, University of Michigan, Ann Arbor, Michigan 48109, United States;* orcid.org/0000-0002-2443-5514; Email: crjsteph@umich.edu

Authors

Cheng Yang − *Willard Henry Dow Laboratory, Department of Chemistry, University of Michigan, Ann Arbor, Michigan 48109, United States*

Gabriel Magallanes − *Willard Henry Dow Laboratory, Department of Chemistry, University of Michigan, Ann Arbor, Michigan 48109, United States;* orcid.org/0000-0003-2097-1325

https://doi.org/10.1021/acs.joc.1c00346
J. Org. Chem. XXXX, XXX, XXX−XXX

Stephen Maldonado − *Willard Henry Dow Laboratory, Department of Chemistry, University of Michigan, Ann Arbor, Michigan 48109, United States; Program in Applied Physics, University of Michigan, Ann Arbor, Michigan 48109, United States;* orcid.org/0000-0002-2917-4851

Complete contact information is available at: https://pubs.acs.org/10.1021/acs.joc.1c00346

Notes

The authors declare no competing financial interest.

■ ACKNOWLEDGMENTS

This work was supported by the National Science Foundation (NSF, No.CHE-1565782) and the University of Michigan. G.M. acknowledges the Rackham Graduate School at the University of Michigan for a Rackham Merit Fellowship.

■ REFERENCES

(1) Corma, A.; Iborra, S.; Velty, A. Chemical Routes for the Transformation of Biomass into Chemicals. *Chem. Rev.* **2007**, *107*, 2411−2502.

(2) Deuss, P. J.; Barta, K. From Models to Lignin: Transition Metal Catalysis for Selective Bond Cleavage Reactions. *Coord. Chem. Rev.* **2016**, *306*, 510−532.

(3) Zakzeski, J.; Bruijnincx, P. C. A.; Jongerius, A. L.; Weckhuysen, B. M. The Catalytic Valorization of Lignin for the Production of Renewable Chemicals. *Chem. Rev.* **2010**, *110*, 3552−3599.

(4) Rahimi, A.; Ulbrich, A.; Coon, J. J.; Stahl, S. S. Formic-acid-induced Depolymerization of Oxidized Lignin to Aromatics. *Nature* **2014**, *515*, 249−252.

(5) Burwell, R. L. The Cleavage of Ethers. *Chem. Rev.* **1954**, *54*, 615−685.

(6) Shuai, L.; Amiri, T.; Questell-Santiago, Y. M.; Héroguel, F.; Li, Y.; Kim, H.; Meilan, R.; Chapple, C.; Ralph, J.; Luterbacher, J. S. Formaldehyde Stabilization Facilitates Lignin Monomer Production During Biomass Depolymerization. *Science* **2016**, *354*, 329−333.

(7) Kärkäs, M. D.; Matsuura, B. S.; Monos, T. M.; Magallanes, G.; Stephenson, C. R. J. Transition-metal Catalyzed Valorization of Lignin: The Key to a Sustainable Carbon-neutral Future. *Org. Biomol. Chem.* **2016**, *14*, 1853−1914.

(8) Zaheer, M.; Kempe, R. Catalytic Hydrogenolysis of Aryl Ethers: A Key Step in Lignin Valorization to Valuable Chemicals. *ACS Catal.* **2015**, *5*, 1675−1684.

(9) Sun, Z.; Fridrich, B.; Santi, A.; Elangovan, S.; Barta, K. Bright Side of Lignin Depolymerization: Toward New Platform Chemicals. *Chem. Rev.* **2018**, *118*, 614−678.

(10) Bosque, I.; Magallanes, G.; Rigoulet, M.; Kärkäs, M. D.; Stephenson, C. R. J. Redox Catalysis Facilitates Lignin Depolymerization. *ACS Cent. Sci.* **2017**, *3*, 621−628.

(11) Lancefield, C. S.; Ojo, O. S.; Tran, F.; Westwood, N. J. Isolation of Functionalized Phenolic Monomers through Selective Oxidation and C-O Bond Cleavage of the β-O-4 Linkages in Lignin. *Angew. Chem., Int. Ed.* **2015**, *54*, 258−262.

(12) Nguyen, J. D.; Matsuura, B. S.; Stephenson, C. R. J. A Photochemical Strategy for Lignin Degradation at Room Temperature. *J. Am. Chem. Soc.* **2014**, *136*, 1218−1221.

(13) Yang, C.; Magallanes, G.; Chan, K.; Stephenson, C. R. J. Organocatalytic Approach to Photochemical Lignin Fragmentation. *Org. Lett.* **2020**, *22*, 8082−8085.

(14) Möhle, S.; Zirbes, M.; Rodrigo, E.; Gieshoff, T.; Wiebe, A.; Waldvogel, S. R. Modern Electrochemical Aspects for the Synthesis of Value-Added Organic Products. *Angew. Chem., Int. Ed.* **2018**, *57*, 6018−6041.

(15) Nguyen, B. H.; Perkins, R. J.; Smith, J. A.; Moeller, K. D. Solvolysis, Electrochemistry, and Development of Synthetic Building Blocks from Sawdust. *J. Org. Chem.* **2015**, *80*, 11953−11962.

(16) Zirbes, M.; Quadri, L. L.; Breiner, M.; Stenglein, A.; Bomm, A.; Schade, W.; Waldvogel, S. R. High-Temperature Electrolysis of Kraft Lignin for Selective Vanillin Formation. *ACS Sustainable Chem. Eng.* **2020**, *8*, 7300−7307.

(17) Rafiee, M.; Alherech, M.; Karlen, S. D.; Stahl, S. S. Electrochemical Aminoxyl-Mediated Oxidation of Primary Alcohols in Lignin to Carboxylic Acids: Polymer Modification and Depolymerization. *J. Am. Chem. Soc.* **2019**, *141*, 15266−15276.

(18) Fang, Z.; Flynn, M. G.; Jackson, J. E.; Hegg, E. L. Thio-assisted Reductive Electrolytic Cleavage of Lignin β-O-4 Models and Authentic Lignin. *Green Chem.* **2021**, *23*, 412−421.

(19) Wu, W.; Huang, J. Electrochemical Cleavage of Aryl Ethers Promoted by Sodium Borohydride. *J. Org. Chem.* **2014**, *79*, 10189−10195.

(20) Roth, H. G.; Romero, N. A.; Nicewicz, D. A. Experimental and Calculated Electrochemical Potentials of Common Organic Molecules for Applications to Single-Electron Redox Chemistry. *Synlett* **2016**, *27*, 714−723.

(21) (a) Hu, P.; Peters, B. K.; Malapit, C. A.; Vantourout, J. C.; Wang, P.; Li, J.; Mele, L.; Echeverria, P.; Minteer, S. D.; Baran, P. S. *J. Am. Chem. Soc.* **2020**, *142* (50), 20979−20986. (b) Shono, T.; Mitani, M. Electroorganic Chemistry. VIII. Intramolecular Cycloaddition of Nonconjugated Olefinic Ketones to Form Cyclic Tertiary Alcohols. *J. Am. Chem. Soc.* **1971**, *93*, 5284−5286. (c) Shono, T.; Nishiguchi, I.; Ohmizu, H.; Mitani, M. Electroorganic Chemistry. 31. Reductive Cyclization of Nonconjugated Olefinic Ketones to Cyclic Tertiary Alcohols. *J. Am. Chem. Soc.* **1978**, *100*, 545−550.

(22) All applied potentials were reported with respect to the standard potential of ferrocenium/ferrocene $E^{0\prime}(Fc^{+}/Fc)$. A hand-made $Ag/AgNO_3$ electrode was used as a reference, and its potential was identified as −0.1 V vs $E^{0\prime}(Fc^{+}/Fc)$.

(23) Assuming reduction of **1a** (0.16 mmol) is one electron process, 1 equiv of electrons (0.16 mmol) = 15.4 Coulombs.

(24) Kärkäs, M. D.; Bosque, I.; Matsuura, B. S.; Stephenson, C. R. J. Photocatalytic Oxidation of Lignin Model Systems by Merging Visible-Light Photoredox and Palladium Catalysis. *Org. Lett.* **2016**, *18*, 5166−5169.

(25) Galkin, M. V.; Sawadjoon, S.; Rohde, V.; Dawange, M.; Samec, J. S. M. Mild Heterogeneous Palladium-Catalyzed Cleavage of β-O-4′-Ether Linkages of Lignin Model Compounds and Native Lignin in Air. *ChemCatChem* **2014**, *6*, 179−184.

(26) Hong, L.; Spielmeyer, A.; Pfeiffer, J.; Wegner, H. A. Domino Lignin Depolymerization and Reconnection to Complex Molecules Mediated by Boryl Radicals. *Catal. Sci. Technol.* **2020**, *10*, 3008−3014.

(27) Hu, Y.; Li, N.; Li, G.; Wang, A.; Cong, Y.; Wang, X.; Zhang, T. Solid Acid-Catalyzed Dehydration of Pinacol Derivatives in Ionic Liquid: Simple and Efficient Access to Branched 1,3-Dienes. *ACS Catal.* **2017**, *7*, 2576−2582.